Cytotoxicity of RH1: NAD(P)H:quinone acceptor oxidoreductase (NQO1)-independent oxidative stress and apoptosis induction

Gabriela Tudor[a], Mike Alley[b], Christopher M. Nelson[c], Ruili Huang[d], David G. Covell[d], Peter Gutierrez[e] and Edward A. Sausville[f]

The elevated expression of the flavoprotein NAD(P)H: quinone acceptor oxidoreductase (NQO1) (EC 1.6.99.2) in many human solid tumors, along with its ability to activate quinone-based anticancer agents, makes it an excellent target for enzyme-directed drug development. Previous studies have shown a significant statistical correlation between NQO1 enzymatic activity and the cytotoxicity of certain antitumor quinones. RH1 [2,5-diaziridinyl-3-(hydroxymethyl)-6-methyl-1,4-benzoquinone], presently in late preclinical and entering early clinical development, has been previously considered to be an excellent substrate for activation by NQO1. In this study we investigate the cytotoxicity of RH1 in cell lines selected from the NCI's 60 tumor cell line panel, expressing varying levels of NQO1 activity. Exposure time- and concentration-dependent cytotoxicity was seen, apparently independent from levels of NQO1 activity in these cells. Furthermore, the NQO1 inhibitor dicoumarol had no impact on the sensitivity profiles of RH1 response. The HL-60 myeloid leukemia cells, which do not have detectable NQO1 activity, were further investigated. RH1 treatment of HL-60 cells generated high levels of free radicals, which was accompanied by robust redox cycling, oxygen consumption and induction of apoptosis. These results are in agreement with previous data suggesting that, in addition to its activation by NQO1, RH1-induced cytotoxicity might involve alternative pathways for activation of this compound. Furthermore, the high cytotoxicity of RH1 in the leukemia/lymphoma subpanel of the NCI *in vitro* cell line screen would suggest an empirical rationale for the utilization of this compound in the treatment of these malignancies. *Anti-Cancer Drugs* 16:381–391 © 2005 Lippincott Williams & Wilkins.

Anti-Cancer Drugs 2005, **16**:381–391

Keywords: antitumor, aziridinylbenzoquinones, apoptosis, free radicals, NQO1, redox cycling

[a]Science Applications International Corp., National Cancer Institute, Frederick, MD, USA, [b]Biological Testing Branch, Developmental Therapeutics Program, DCTD, National Cancer Institute, Frederick MD, USA, [c]Johns Hopkins University, Baltimore MD, USA, [d]Screening Technologies Branch, Developmental Therapeutics Program, National Cancer Institute, Frederick MD, USA, [e]University of Maryland Greenebaum Cancer Center, Baltimore MD, USA and [f]Developmental Therapeutics Program, DCTD, National Cancer Institute, Rockville, MD, USA.

Sponsorship: This project has been funded with Federal funds from the National Cancer Institute, National Institute of Health, under contract N01-C0-56000.

Disclaimer: The content of this publication does not necessarily reflect the views or policies of the Department of Health and Human Services nor does mention of trade names, commercial products or organizations imply endorsement by the US Government.

Correspondence to E. A. Sausville, University of Maryland Greenebaum Cancer Center, 22 S. Greene Street, Baltimore, MD 21201-1595, USA.
Tel: +1 410 328-7394; fax: +1 410 328-6896;
e-mail: esausville@umm.edu

Received 6 June 2004 **Revised form accepted** 2 December 2004

Introduction

NAD(P)H:quinone acceptor oxidoreductase (NQO1) is one of several reductase enzymes capable of reducing quinones to DNA-damaging species. Other reductases including NADPH cytochrome P450 and NADH cytochrome b_5 reductase have also been associated with the metabolism of quinones. NQO1 catalyzes the two-electron reduction of quinones to their hydroquinone derivatives, bypassing the semiquinone intermediates [1]. This reaction prevents the one-electron reduction, which would result in oxidative cycling, generation of free radicals and oxidative stress. However, the reduced hydroquinones can rapidly autoxidize and undergo redox cycling generating intermediate radical species. These radical metabolites have been shown to induce cellular damage by acting as alkylating agents and/or by inducing oxidative stress [2–4]. Examples of compounds that have been shown to be good substrates for NQO1 include indoloquinone EO9 [5], mitomycin C [2,4,6–8], streptonigrin [9], MeDZQ [3,10] and diaziquone [11,12]. The high level of NQO1 in tumor tissue, as compared to normal tissue [13,14], has made NQO1 a useful target for quinone-based bioreductive antitumor therapies [15].

RH1 [2,5-diaziridinyl-3-(hydroxymethyl)-6-methyl-1,4-benzoquinone], a water-soluble analog of MeDZQ (3,6-dimethyl-2,5-diaziridinyl-1,4-benzoquinone) [10,16–25], is an antitumor agent undergoing late preclinical and early clinical studies. Prior work had suggested that RH1 is highly active and selectively toxic to cells with elevated

0959-4973

NQO1 activity, and has pharmacological properties different from other aziridinylquinones, e.g. EO9 [19,23]. *In vitro* studies with purified human NQO1 and HPLC [16,19] have shown that RH1 is rapidly reduced by NQO1 to the hydroquinone. It is commonly accepted that the antitumor activity of DZQ, MeDZQ and RH1 is mainly the result of their two-electron reduction by NQO1 to DNA-alkylating aziridinylhydroquinones [26–28]. Indeed, the sensitivity of a large number of different cell lines to MeDZQ, RH1 or EO9 increased with an increased level of NQO1 expression [15,16,20,29]. Whether additional pathways for RH1 metabolism independent of NQO1 are important in activation of the drug remains incompletely explored.

In this study we determined the sensitivity to RH1 of tumor cell lines differing in NQO1 activity levels, on the background of varying levels of other enzymes possibly involved in aziridinylquinone metabolism [28]. This approach becomes meaningful in the context of the clinical evaluation of these compounds, since tumor sensitivity to bioreductive agents *in vivo* is likely to be affected by several bioreductive enzymes.

Our study shows that although it is certainly true that sensitivity to RH1 was marked in cell lines expressing NQO1, the capacity of RH1 to convey cytotoxicity did not correlate in a dependent fashion with the levels of NQO1 activity. Furthermore, dicoumarol, a NQO1 inhibitor, had very little if any impact upon the sensitivity profiles of RH1 treatment. The activity of RH1 in the HL-60 myeloid leukemia cells, which do not have detectable NQO1 activity [28,30], was further investigated. RH1 treatment generated high levels of free radicals, which was accompanied by robust redox cycling, oxygen consumption and induction of a high level of apoptosis. These results are in agreement with previous data suggesting that, in addition to its activation by NQO1, RH1 cytotoxicity might involve alternative or additional pathways of activation to NQO1. Furthermore, the high sensitivity of the leukemia/lymphoma cell lines to RH1 would support the use of this compound as a potential drug for the treatment of leukemias, even without NQO1 expression.

Materials and methods

Materials

Compounds were obtained from the NCI Open Compound Repository, Drug Synthesis and Chemistry Branch, NCI. Stock solutions of drugs were made in dimethylsulfoxide (DMSO) and stored at −70°C. The spin trap 5,5-dimethyl-1-pyrroline-*N*-oxide (DMPO) was obtained from Aldrich (St Louis, MO). 6-Carboxy-2′,7′-dichlorodihydrofluorescein diacetate, di(acetoxymethyl ester) (CM-H_2DCFDA) and hydroethidium (HE) were from Molecular Probes (Eugene, OR).

In vitro 60 cell line cancer screen

The methods used for the 60 cell line panel have been described elsewhere [31,32]. Briefly, compounds were solubilized in DMSO at a final concentration of 200×. The compounds were diluted into RPMI 1640 containing 5% fetal bovine serum (FBS) and serial 1-log dilutions were prepared for a total of five concentrations. Generally, the working range for the initial testing of a compound was 10^{-4} through 10^{-8} M. The compounds were added to 24-h-old cultures of each of the 60 cell lines used in the panel. Following a 48-h incubation, the media was removed, the cells fixed and stained with sulforhodamine B, and the total stain quantitated by optical density determinations. Through the use of a time 0 cell control, cell growth could be determined for each cell line, thus allowing calculations of the 50% growth inhibitory concentration (GI_{50}), the total growth inhibition (TGI) and the 50% lethal concentration (LC_{50}). These data could then be plotted as mean bar graphs, where the average GI_{50}, TGI and 50% cell kill (LC_{50}) were computed, and the susceptibility of individual cell lines represented as bars to the right indicating sensitivity greater than the mean and to the left indicating resistance relative to the mean.

In vitro time course assay

Methods for cell culture, drug preparations and conventional *in vitro* drug sensitivity testing have been described previously [33]. The cell lines and concentration ranges of experimental agents to be evaluated in the more specialized concentration × time ($c \times t$) assays were chosen on the basis of 60 cell line screening data. As described elsewhere [34,35], exposure to an experimental agent for increasing periods of time, followed by drug removal, permits quantitation of drug activity conferred by each of several exposure durations ranging from less than 1 to 144 h. Comparison to plates not exposed to drug permits determination of concentration and times of exposure conferring GI_{50}, TGI and LC_{50}. From the plotting of composite $c \times t$ data, one can readily determine the minimum exposure conditions (both concentration and time) required to achieve cytostatic and/or cytocidal activity in a given cell line, and then compare the relative sensitivities of multiple cell lines to identify the most sensitive cell types.

Electron spin resonance (ESR) measurements

To characterize the capacity of RH1 and EO9 to participate in oxygen-mediated bioactivation steps, ESR spectra were obtained at room temperature using a Varian E109 Century Series ESR spectrometer (Varian, Palo Alto, CA) equipped with 100-kHz field modulation, as previously described [30]. Briefly, 1×10^7 cells were rapidly mixed with 1 mM compound and 100 mM of the spin trap DMPO. The high concentrations of drug, clearly above the concentrations which cause lethality by both RH1 and EO9, were necessary to adequately characterize

initial rates of radical generation. The drug-loaded cells were quickly transferred to an ESR flat cell and placed in the ESR spectrometer for measurement. Control experiments were carried in the absence of drug. The relative ability of the various quinones to produce hydroxyl radicals was evaluated by using the steady-state signal intensity of the DMPO-OH adduct.

Oxygen consumption measurements

The rate of oxygen consumption was determined on whole cells with a Model 53 Oxygen Monitor (Yellow Springs Instruments, Yellow Springs, OH). Exponentially growing cells were harvested and suspended to a density of 10^7 cells/ml. An aliquot of 3 ml of cell suspension was aerated in the receptacle of the Model 53 oxygen monitor for 3 min and the oxygen consumption evaluation was based on a 100% value of 1.58×10^{-7} mol/ml of dissolved oxygen. Endogenous cellular oxygen consumption was monitored for 5 min before drugs were added. Drug-induced oxygen consumption was monitored by recording the drop in oxygen saturation levels for an additional 5 min after addition of the drug (1 mM final concentration from stock solutions in DMSO) and without drug. The rate of drug-induced oxygen consumption was calculated and expressed as the ratio of $[O_2]_{drug}/[O_2]_{control}$.

Detection of peroxides and superoxides by flow cytometry

To verify the production of reactive oxygen species (ROS) at more pharmacologically relevant concentration ranges, HL-60 and MCF-7 cells (1×10^6 cells) were incubated with drug following the same conditions used for the apoptosis assay. DCFH-DA and HE were dissolved in DMSO and incubated with the cells for 30 min at 37°C. Following incubation, the medium was removed and the cells were analyzed with a FACScan (Becton Dickinson, Mountain View, CA). The non-enzymatic decomposition of H_2O_2 (20 mM) with generation of hydroxyl radicals was used as a positive control for the detection of peroxides. Hydroquinone and thiotepa were used as positive and negative controls, respectively.

Apoptosis assay

Apoptosis was detected by flow cytometry using the Annexin-V–FITC apoptosis detection kit from Oncogene Research Products (San Diego, CA). Cells were incubated with drug for 0, 3, 6 and 24 h at concentrations higher than TGI. Following drug treatment, 5×10^5 cells were used for the conventional Annexin-V-binding protocol, according to the manufacturer's instructions and bivariate Annexin-V/propidium iodide (PI) analysis was performed by flow cytometry.

Western blot analysis

The Western blot analysis was performed as described previously [30]. Briefly, 1×10^7 cells were harvested and lysed by homogenization. Cell homogenates were centrifuged at 14 000 *g* for 30 min at 4°C. Supernatants were collected and stored at −70°C, until analyzed by gel electrophoresis. These lysates contained the cytosolic and light membrane fractions but not nuclei or mitochondria. Protein content in each lysate was determined by using the BCA Protein Assay (Pierce, Rockford, IL). The following primary antibodies were used: β-actin, mouse monoclonal (Sigma, St Louis, MO; A5441), cytochrome *c*, mouse monoclonal (PharMingen, San Diego, CA) and PARP mouse polyclonal (BD Biosciences, Mountain View CA; 65196E). The resulting immunoblot signals were quantified by densitometric scanning (Digital Imaging System; Alpha Innotech, San Leandro, CA). The β-actin signal was used to normalize for the amount of protein loaded in each lane.

Results

RH1 sensitivity profile in the 60 cell line screen

RH1 (NSC 697726) demonstrated potent yet differential (some cell types much more sensitive than others) activity in the NCI 60 cell line screen. The initial testing of RH1 in seven separate experiments over a concentration range of 0.01–100 μM resulted in a mean GI_{50} of 0.025 μM, a mean TGI of 0.338 μM and a mean LC_{50} of 7.3 μM (population variances 0.3, 0.9 and 0.9, respectively) for the conventional 2-day assay. Many individual cell lines in the leukemia, lung, colon, CNS, melanoma, ovary, breast and renal subpanels exhibited differentially greater sensitivities such that TGI and LC_{50} values were 1.25–1.53 logs more or less sensitive than the 60 cell line mean values. Subsequent testing of RH1 over a lower concentration range of 0.1–1000 nM resulted in a more accurate determination of the GI_{50} sensitivity pattern of the 60 cell lines. As shown in Figure 1, under conditions of a 2-day assay, the mean GI_{50} was measured to be 12 nM with leukemia cell lines exhibiting the greatest differential GI_{50} sensitivities ranging from 0.14 to 1.0 nM (1.09–1.94 logs more sensitive than the 60 cell line mean panel value).

$c \times t$ sensitivity profiles of RH1

In vitro time course assays initially were performed on RH1 in selected lung and breast tumor cell lines in order to characterize and compare the time and concentration dependency of this agent, and to help select an optimal *in vivo* drug treatment schedule in sensitive tumor models. As shown in Figure 2, most of the solid tumor cell lines required a minimum of 12 h to achieve near maximum activity on a $c \times t$ basis. *In vitro* time course assays also were employed to compare the relative efficacy of RH1 with other structural analogs, i.e. mitomycin C, diaziquone and EO9 (concurrent testing). As shown in Table 1, RH1 is generally the most active structure on a molar basis in culture.

Fig. 1

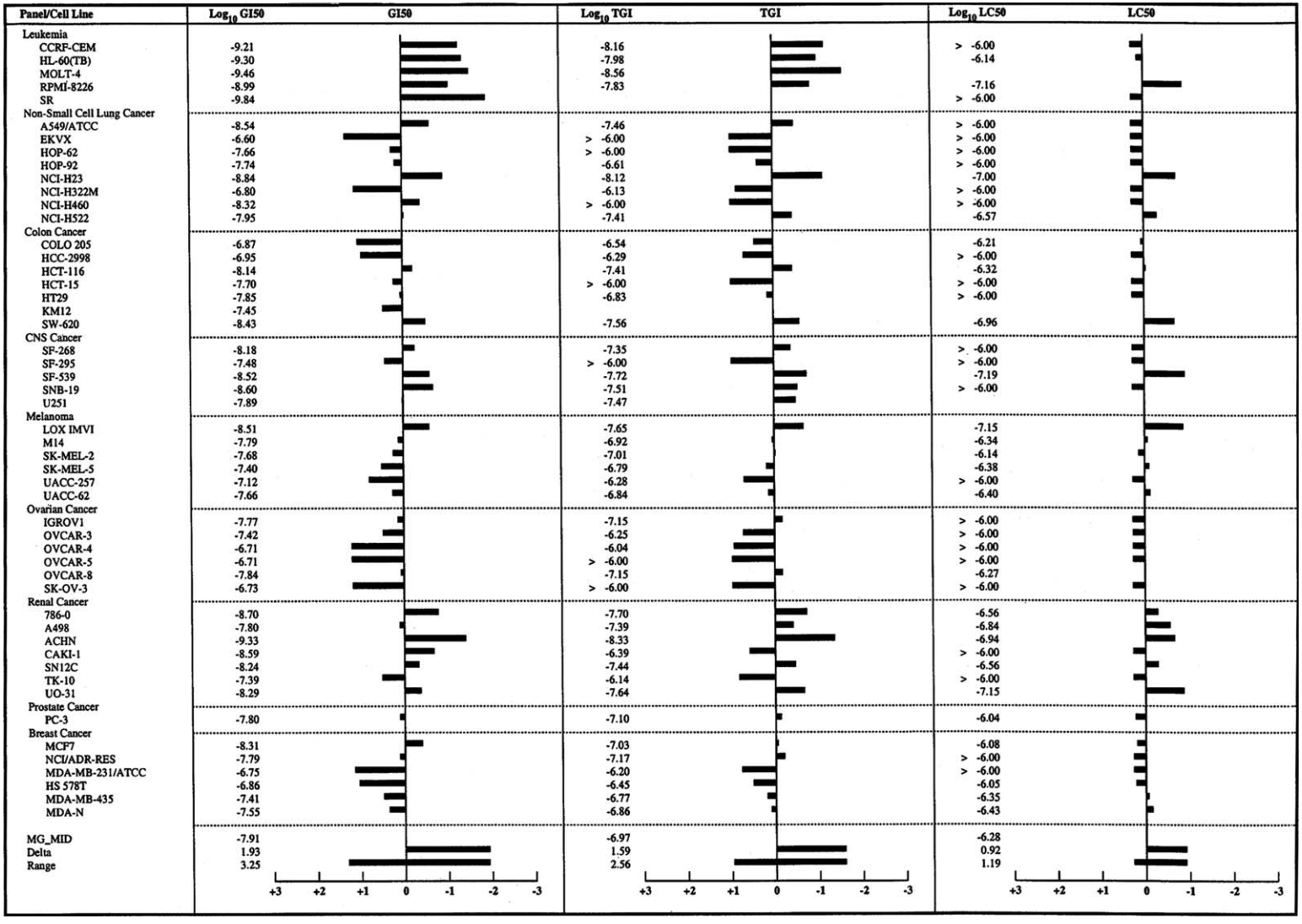

RH1 activity in the NCI 60 cell line screen. Mean graphs of the RH1 (NSC 697726) activity (log_{10} of molar concentration) in the NCI 60 cell line screen, as described in Materials and methods. Note that bars projecting to the right indicate drug activity greater than the mean value and bars projecting to the left indicate drug activity less than the mean value. MG_MID = the mean activity value for the entire panel, Delta = the number of log_{10} units by which values for the individual cell lines differ (plus or minus) from the MG_MID value of the panel and Range = the number of log_{10} units by which the value for the cell line with the highest sensitivity to the drug differs from the line with the lowest sensitivity.

Fig. 2

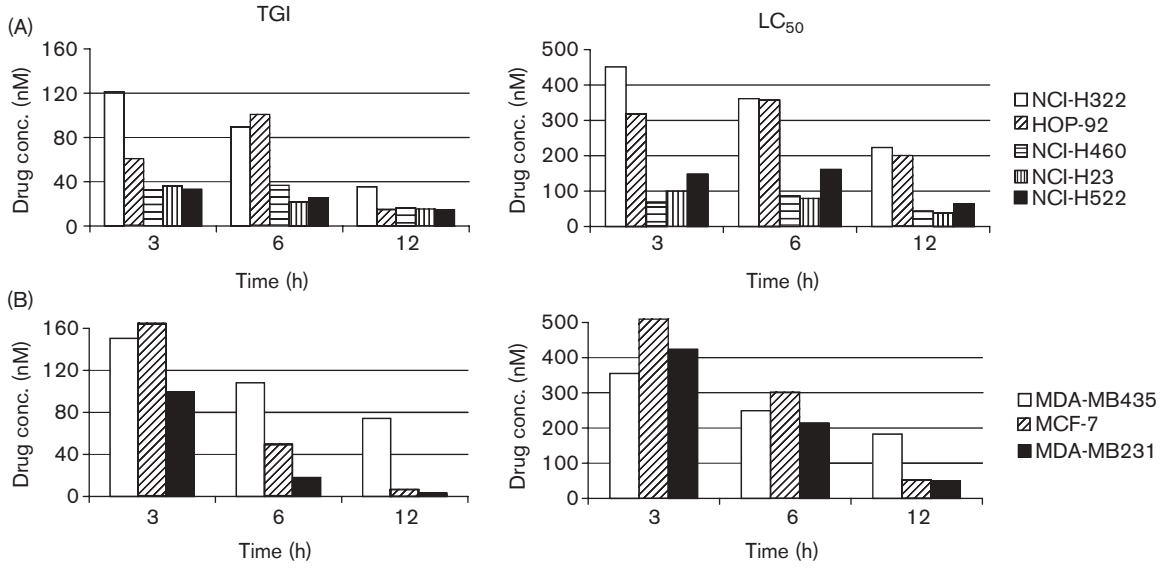

Indices of sensitivity to RH1. Drug sensitivity is expressed as TGI (left panels) and LC_{50} (right panels) as described in Materials and methods. The *in vitro* time course assay was performed on selected lung (A) and breast (B) tumor cell lines. The data represent mean TGI and LC_{50} values following treatment with nanomolar concentrations of RH1 from triplicate samples and two different experiments.

Table 1 Pharmacologic indices (nM) for potential NQO1 substrate agents following 6 days continuous exposure in the NCI 60 cell anticancer drug screen

Cell line/indices	MITC	AZQ	EO9	RH1
NCI-H23				
GI_{50}	29.3	196	1.5	1.7
TGI	68.8	509	2.8	3.6
LC_{50}	206	2520	14	8
NCI-H522				
GI_{50}	6.4	24.5	1.2	0.2
TGI	12	70.8	1.6	0.7
LC_{50}	73.9	834	14	8
MDA-MB231				
GI_{50}	224	386	28	3.5
TGI	1190	1260	122	12.3
LC_{50}	4670	2970	260	31.4

Sensitivity of tumor cell lines to selected quinone-based compounds following 6 days of continuous exposure as described in Materials and methods. Data correspond to the mean indices of three independent experiments and represent nanomolar concentrations of drug.

The prominent RH1 sensitivity of different leukemia or lymphoma cell lines in the 60 cell line screen prompted further time course assay evaluations in leukemia/myeloma cell lines: CCRF-CEM, Molt-4, HL-60TB and RPMI-8226.

In contrast to the time and concentration dependence of most of the solid tumor cell lines, which achieve near maximum LC_{50} level of activity within 6- to 12-h exposures as shown in Figure 2, leukemia cell lines were highly responsive to brief exposures and low drug concentrations as shown in Figure 3.

Correlation of RH1 activity with NQO1 (DT-diaphorase) expression

As prior experiments had indicated that one route to bioactivation of RH1 utilized NQO1 and as prior studies had characterized NQO1 expression in the NCI 60 cell line screen, it became of interest to correlate RH1 activity with expression of NQO1. Figure 4 shows the lack of significant correlation between susceptibility to RH1 and expression of NQO1. In fact, of great interest, this analysis revealed that HL60 leukemia cells showed high susceptibility to RH1 despite essentially no detectable NQO1 activity [28,30]. Real-time quantitative PCR analysis of HL60 cells did not reveal any induction of NQO1 expression following treatment with RH1 (manuscript in preparation). We therefore sought to indirectly characterize NQO1 activity in relation to RH1-induced cytotoxicity by use of dicoumarol. Although dicoumarol is not a very specific inhibitor of NQO1, it is commonly used as an indicator of NQO1 participation in a redox mechanism. Figure 5 shows the sensitivity profiles (TGI) of cell lines in response to RH1 and co-treatment with increasing concentrations of dicoumarol. The sensitivity to RH1 does not decrease (Fig. 5B) in the presence of dicoumarol in cell lines with intermediate/high levels of endogenous NQO1 activity (activity $\log_{10}$: NCI-H522 = 2.54, NCI-H460 = 3.78 and MCF-7 = 1.81) [28]. As expected, there is no influence of dicoumarol on the sensitivity of the leukemia cell lines (Fig. 5A) that contain no NQO1 activity [28].

Fig. 3

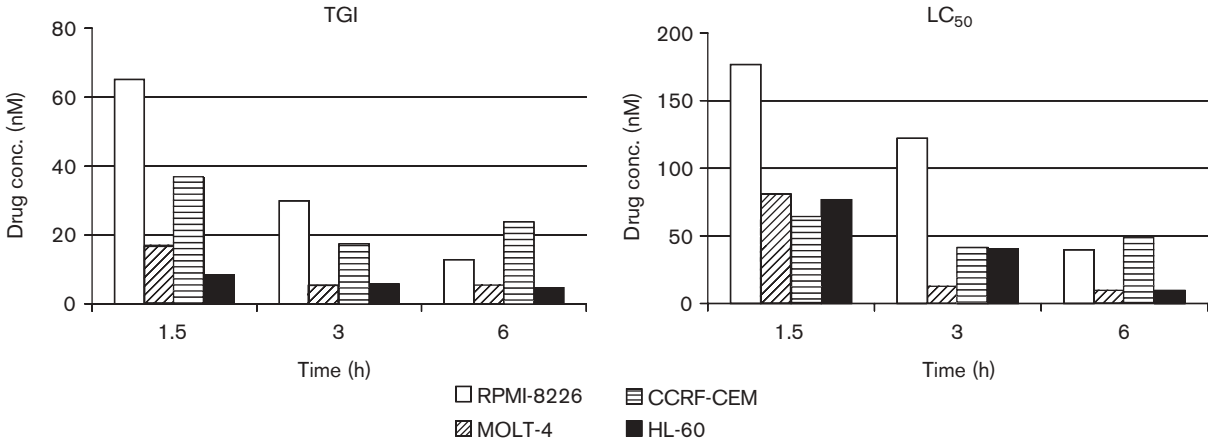

Indices of sensitivity to RH1. Drug sensitivity is expressed as TGI (left panel) and LC_{50} (right panel) as described in Materials and methods. The *in vitro* time course assay was performed on selected leukemia/lymphoma cell lines. The data represent mean TGI and LC_{50} values following treatment with nanomolar concentrations of RH1 from triplicate samples and two different experiments.

Fig. 4

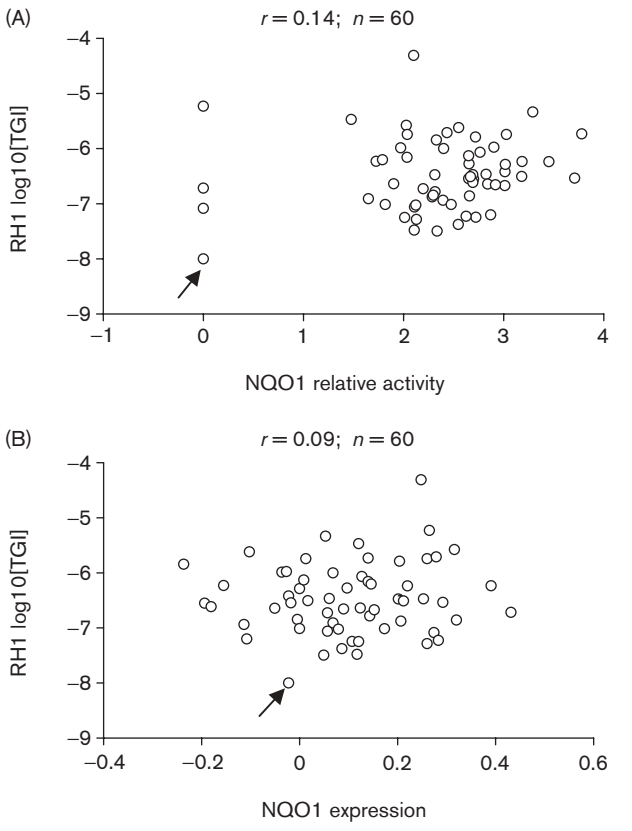

Statistical correlation between sensitivity to RH1 (TGI) and NQO1 activity. (A) NQO1 enzyme activity [28] and (B) NQO1 log (mRNA) expression (microarray data/molecular target 22/MT22) correlation in the 60 cell line panel of the NCI *in vitro* anticancer drug screen (http://dtp.nci.nih.gov). Arrows indicate the HL60 cell line.

Detection of drug-induced free radicals and oxygen consumption in whole cells

One-electron reduction of quinones generates a semiquinone intermediate, which under aerobic conditions is oxidized to the parent quinone, a process known as redox cycling, that results in the concomitant production of superoxide radical anion. The formation of superoxide is the beginning of a cascade that generates hydrogen peroxide and hydroxyl radicals [36,37]. In the case of a two-electron reduction by NQO1, the hydroquinone is produced. If the hydroquinone is unusually stable, redox cycling will not take place sparing the cells from oxidative stress. Hydroquinones, however, can also be oxidized by one electron at a time with the formation of the semiquinone and the parental compound, and generation of ROS [12,37,38]. These characteristics are well defined in purified enzyme systems. In whole cells, however, both one- and two-electron reductions lead to more complicated chemical reactions.

NQO1-catalyzed reduction of aziridinylbenzoquinones has been reported to result in the formation of ROS [25,30,38]. However, the auto-oxidation of two-electron reduced RH1 has been reported to be slow [25] (reoxidation half-time around 40 min), suggesting that this role of NQO1 in the oxidative stress induced by RH1 might be negligibly low. We therefore sought to characterize the generation of reactive oxygen intermediates following exposure of both RH1 and EO9 to cells with low/absent (HL-60 leukemia) and intermediate/high (MCF-7 breast carcinoma) NQO1 activity. The spin trap DMPO was used to detect the production of hydroxyl radicals through formation of its hydroxyl radical adduct DMPO-OH, which is at the end of the cascade

Fig. 5

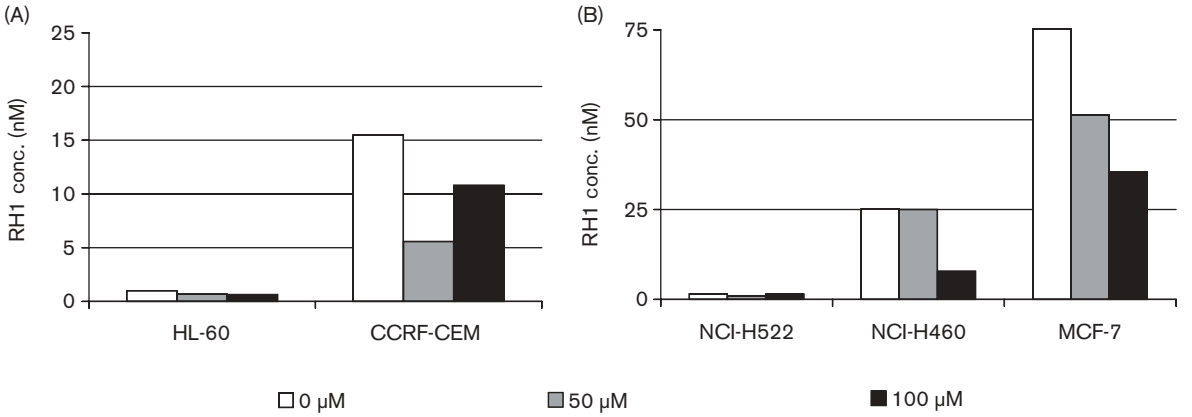

Indices of sensitivity to RH1 and dicoumarol co-treatment. The *in vitro* time course assay was performed on selected leukemia/lymphoma (A) and lung/breast (B) cell lines as described in Materials and methods. The data represent mean TGI values following co-treatment for 24 h with nanomolar concentrations of RH1 and 0 (white bars), 50 (grey bars) or 100 μM (black bars) dicoumarol, from triplicate samples and two different experiments.

Table 2 Comparison of hydroxyl radical formation and oxygen consumption mediated by quinone-based agents in whole MCF-7 and HL-60 cells

Group	NSC	DMPO-OH (arbitrary units)			$[O_2]_{D/C} \pm SD$
		4 min	8 min	12 min	
HL-60 cells					
RH1	697726	11.0	24.0	23.5	2.83 ± 0.24
EO9	382459	17.0	9.5	9.0	1.92 ± 0.09
MCF-7 cells					
RH1	697726	18.0	27.0	34.0	2.04 ± 0.27
EO9	382459	19.0	22.0	20.0	1.35 ± 0.08

ESR data is the signal intensity observed for the DMPO-OH adduct determined by measuring the peak to peak height of the second low field line of the DMPO-OH adduct spectrum, at 4, 8 and 12 min after the onset of the reaction. Oxymetry data are the oxygen consumption rates (D/C) obtained by measuring the drop in intracellular oxygen levels in drug-treated (D) and untreated (C) cells. Values are mean of duplicate determinations.

started by superoxide. ESR spectra were generated and the DMPO-OH adduct formation analyzed as previously described [30]. Because the compounds were dissolved in DMSO, this solvent provided an internal control used to eliminate the possibility of artifacts involved in the production of the observed DMPO-OH adduct, such as rearranging of the DMPO-superoxide adduct. The hydroxyl radicals react with DMSO producing a carbon-centered radical, which is then trapped by DMPO with generation of characteristic ESR spectra, as previously shown [30]. The oxygen consumption rate reflects the rate of redox cycling and the rate at which oxygen is being consumed. Table 2 summarizes the data generated by these two analytical methods. Despite marked differences in levels of NQO1 expression in MCF-7 and HL-60, there is little variation in the bioactivation of these two aziridinylbenzo-quinones in the two cell lines. Based on oxygen consumption rates and hydroxyl radical concentrations, EO9 appears to redox cycle better in HL-60 in comparison to MCF-7 cells. In HL-60 cells, EO9 appears to be rapidly metabolized, most probably by one-electron reduction. RH1, instead, shows higher levels of hydroxyl radicals than does EO9 in the HL-60 cells. This correlates well with the higher cytotoxicity of RH1 in this cell line. Furthermore, the hydroxyl radical concentrations generated by RH1 in the HL-60 cells are similar to those generated in the MCF-7 cells, in spite of their differences in NQO1 activity and cytotoxicity profile. The slower metabolic rate of the RH1 in both cell lines would suggest a more stable metabolic intermediate.

We also used a different approach to confirm free radical generation by RH1 in HL-60 leukemia cells at more pharmacologically relevant concentrations than those studied in the ESR experiments. We detected intracellular ROS as a function of drug concentration and time of exposure by flow cytometry, using the fluorescent dye H_2DCF-DA for the detection of peroxides and HE for the detection of superoxides (Fig. 6). Thiotepa, *N*,*N*′,*N*″-triethylene thiophosphoramide, an alkylating agent containing the aziridinyl group, was used as negative control for ROS generation and hydroquinone, 1-4-benzenediol, was used as a positive control. The response of HL-60 cells to RH1 treatment was time and concentration dependent, with a peak for superoxide generation occurring at 6 h (Fig. 6A). The generation of peroxides was evident by 3 h after increasing the drug concentration to 40 nM (Fig. 6B). EO9, instead, generates ROS as early as 3 h, although a 1 μM concentration was necessary to detect similar levels of ROS. This is in agreement with faster metabolism of EO9 and higher cytotoxicity of RH1 in the HL-60 cells.

Fig. 6

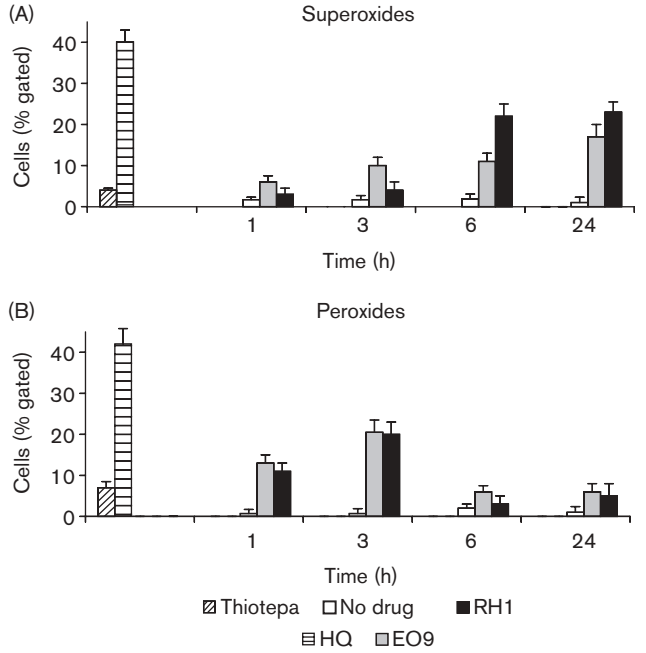

ROS detection as DCFDA and HE oxidation in the HL-60 cells by flow cytometry. One million cells were treated with drug for 1, 3, 6 and 24 h, followed by a 30-min treatment with DCFDA and HE. EO9 was used at 1 μM concentration and RH1 at 20 nM for the detection of superoxides, and at 40 nM for the detection of peroxides. Control agents are hydroquinone at 50 μM for 1 h treatment and thiotepa at 200 μM for 24 h treatment. Data represent the bivariate flow cytometric analysis expressed as percentage of cells showing a positive signal. Values are means from three separate experiments.

Fig. 7

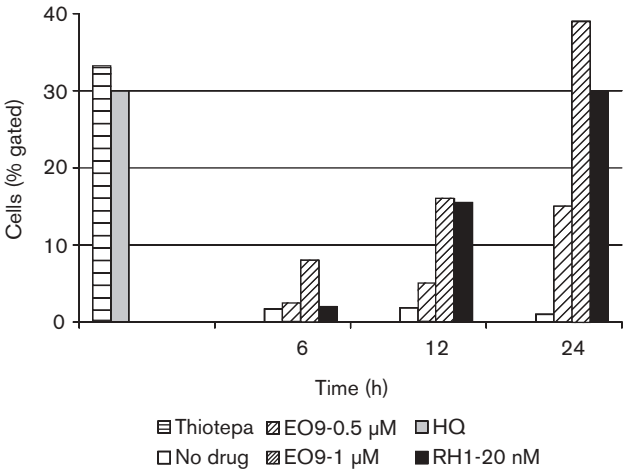

Apoptosis detection in the HL-60 cells treated with RH1 and EO9. Apoptosis was measured by double staining with Annexin-V and PI. Cells were treated with RH1 at 20 nM and EO9 at 1 μM for 6, 12 and 24 h, and stained with Annexin-V/PI according to the manufacturer's instructions. Data represent the percentages of Annexin-V^+ and PI^- cells. Positive controls for apoptosis are thiotepa at 200 μM for 24 h treatment and hydroquinone at 50 μM for 3 h treatment. Values are means from three separate experiments.

Induction of apoptosis in HL-60 cells

We measured apoptosis by assessing the externalization of phosphatidylserine (PS) by double staining with Annexin-V and PI. The percentages of Annexin-V^+/PI^- cells are shown in Figure 7. RH1 induces substantial levels of apoptosis in the HL-60, beginning at 12 h and reaching high levels at 24 h. This is in agreement with the ROS generated in response to RH1, at these concentrations. EO9 instead, requires higher concentrations (1 μM) to induce similar levels of apoptosis. The earlier detection of ROS induced by EO9 also correlates with earlier induction of apoptosis.

During the late stages of apoptosis, p85, the cleavage product of PARP-1, has been reported to migrate from the nucleus into the cytoplasmic/perinuclear region [39]. As shown in Figure 8, in cells treated with EO9, the 85-kDa fragment is greatly increased at 24 h and is preceded by an early increase in cytochrome *c* release into the cytosol. In contrast, RH-1 treatment causes only partial enrichment in p85, which is not accompanied by a noticeable increase in cytochrome *c* release. These findings raise the possibility that EO9 induces apoptosis by prominently activating a caspase/PARP-mediated pathway leading to release of cytochrome *c*, while RH1-mediated growth inhibition and apoptosis proceeds through a mechanism that does not as prominently depend on this apoptotic program.

Discussion

We demonstrate here that RH1 is a potent inhibitor of cell growth in the NCI 60 cell line anticancer drug screen and that relatively short periods of exposure to submicromolar concentrations are capable of causing induction of apoptosis, particularly of leukemia cell lines. Surprisingly, RH1 cytotoxicity appeared to be potently induced in cells with low to absent expression of the activating enzyme NQO1. Even in cells lacking NQO1 expression, RH1 displayed robust O_2 consumption, and had evidence of superoxide and peroxide production. As a major basis for the cytotoxic effects of aziridinylbenzoquinones had previously been attributed to two-electron reduction to alkylating products by NQO1, one strategy for clinical trials with RH1 might use NQO1 expression as a basis for selecting patients whose tumors might respond to RH1.

Opposing the idea that NQO1 expression should be a basis for patient selection is the evidence that autooxidation and redox cycling of semiquinone or hydroquinone forms generated by two-electron reduction has also been reported as an important factor in aziridinyl-

Fig. 8

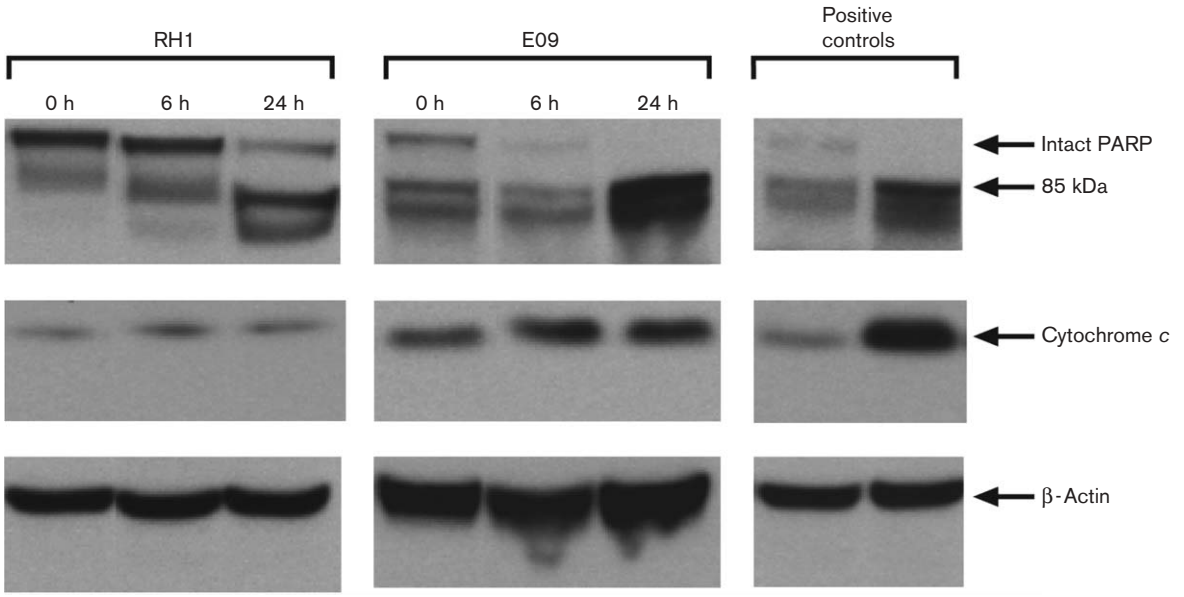

p85 enrichment and cytochrome *c* release in the cytosol of HL-60 cells following treatment with RH1 and EO9. Cells were treated with RH1 at 20 nM and EO9 at 1 μM for 3, 6 and 24 h. Lysates were prepared and assessed by immunoblot as described in Materials and methods. The positive control for PARP-1 cleavage is HL-60 cells treated with hydroquinone at 50 μM for 3 h (right lane) as compared to untreated cells (left lane). The positive control for cytochrome *c* release is HL-60 cells treated with thiotepa at 200 μM for 24 h (right lane) as compared to untreated cells (left lane).

benzoquinone-mediated cytotoxicity. For example, flavoenzyme electron transferases may reduce aziridinyl-substituted quinones in a single-electron way to their radicals, which further undergo redox cycling or possibly may alkylate DNA [25,27,40]. Conflicting results have emerged from the study of isogenic lines engineered to express differing levels of NQO1 [20,22]. In one of the isogenic models [20] the expression of NQO1 protein did not affect the activity of RH1 in these cells following a 96-h drug treatment.

The experiments reported here demonstrate that the aziridinylbenzoquinone RH1 is active in different cell lines in a way that appears not to correlate with NQO1 activity levels. RH1 has been reported to be a very good substrate for the NQO1 reductive activation. Our results emphasize that alternative mechanisms of activation have been suggested. Among these, oxidative stress, presumably initiated by single-electron transferring flavoenzymes, appears to be an important mechanism of cytotoxicity of aziridinylbenzoquinones, although where NQO1 is present, it certainly could contribute to RH1 bioreductive activation and could conceivably contribute to cytotoxicity perhaps over and above that due to redox cycling ability. Among the cell lines tested in this study, the leukemia/lymphoma cell lines, which express low levels of NQO1 activity, demonstrate the highest sensitivity to RH1. Furthermore, the sensitivity of cell lines with varying levels of NQO1 activity is not compromised by cotreatment with dicoumarol.

We have previously shown that among quinones, whose cytotoxicity appears to correlate directly with the expression of high levels of NQO1, the aziridinylbenzoquinones show superior cytotoxicity, which, however, does not correlate simply with high levels of ROS generated from their metabolism. Recently, it has been shown that NQO1 activates RH1 to a potent DNA cross-linking species [22]. Thus, in addition to generation of ROS, the aziridine and hydroxyl groups may contribute to activation of an alkylating species after reduction [41]. In order to evaluate the reactivity of RH1 as a substrate for bioreductive activation, we looked at the levels of free radicals generated as a contribution of the one- and two-electron reductive mechanisms in the MCF-7 and HL-60 cells. The redox cycling of RH1 and EO9, another substrate for NQO1, generated high levels of hydroxyl radicals in the HL-60 and MCF-7 cells, despite the fact that NQO1 is essentially absent in HL60. However, the cytotoxicity of RH1 in the HL-60 cells is considerably higher, which would suggest additional factors contributing to the RH1 cytotoxicity in these cells.

In addition to reductases [28], HL-60 cells are known to contain high levels of myeloperoxidase (MPO), which can bioactivate hydroquinones to their reactive quinone

metabolites, resulting in cellular damage and apoptosis, including activation of caspases. EO9 requires much higher concentrations and is rapidly metabolized in the HL-60 cells, perhaps indicating a preferred one-electron reductive pathway, which in the MCF-7 cells might compete with the two-electron reductive pathway. In the final analysis, the observed data suggest that RH1, in addition to being a substrate for two-electron reductions with the production of hydroquinone, can also be reduced by non-NQO1 reductases, which ultimately results in the generation of free radicals, oxidative stress to the cells and major cytotoxicity.

These results do not rule out the contribution of bioreductive activation of antitumor quinones by NQO1 in cells with high baseline levels of NQO1. However, our results suggest that NQO1 activity should not be considered a prerequisite for potential activation by NQO1. In fact, our data clearly provide a basis for interest in clinical trials of RH1 in patients with relapsed and refractory hematopoietic malignancies. The pathways activated by RH1 leading to apoptosis will need clarification in future experiments. The most common pathway for induction of apoptosis involves mitochondrial damage, release of cytochrome *c* and/or activation of caspases, although the activation of apoptotic pathways bypassing cytochrome *c* release or activation of caspases has also been reported [42,43]. The lack of significant release of cytochrome *c* into the cytosol in response to the aziridinylquinones as compared to the other quinones [30] has suggested the activation of separate signaling pathways leading to apoptosis. We demonstrate here that although RH1 more potently induces apoptosis in HL-60 cells as compared to EO9, it shows only limited or no release of cytochrome *c*, which would suggest an alternative apoptotic pathway. Therefore, these experiments raise the hypothesis that RH1 activates pro-apoptotic signals in a way that qualitatively differs from EO9 and which may be influenced by, but not depend on, the background levels of NQO1 expression. Future experiments will address the apoptotic mechanisms induced by RH1.

References

1 Ernster L. DT-diaphorase. *Methods Enzymol* 1967; **10**:309–317.
2 Siegel D, Gibson NW, Preusch PC, Ross D. Metabolism of mitomycin C by DT-diaphorase: role in mitomycin C-induced DNA damage and cytotoxicity in human colon carcinoma cells. *Cancer Res* 1990; **50**:7483–7489.
3 Gibson NW, Hartley JA, Butler J, Siegel D, Ross D. Relationship between DT-diaphorase-mediated metabolism of a series of aziridinylbenzoquinones and DNA damage and cytotoxicity. *Mol Pharmacol* 1992; **42**:531–536.
4 Ross D, Siegel D, Beall HD, Prakash AS, Mulcahy RT, Gibson NW. DT-diaphorase in activation and detoxification of quinines. Bioreductive activation of mitomycin C. *Cancer Metastasis Rev* 1993; **12**:83–101.
5 Walton MI, Bibby MC, Double JA, Plumb JA, Workman P. DT-diaphorase activity correlates with sensitivity to the indoloquinone E09 in mouse and human colon carcinomas. *Eur J Cancer* 1992; **28A**:1597–1600.
6 Gan Y, Mo Y, Kalns JE, Lu J, Danenberg K, Danenberg P, Wientjes MG, *et al.* Expression of DT-diaphorase and cytochrome P450 reductase correlates with mitomycin C activity and human bladder tumors. *Clin Cancer Res* 2001; **7**:1313–1319.
7 Wang X, Doherty G, Leith M, Curphey T, Begleiter A. Enhanced cytotoxicity of mitomycin C in human tumour cells with inducers of DT-diaphorase. *Br J Cancer* 1999; **80**:1223–1230.
8 Siegel D, Hartman C, Beall H, Kasai M, Arai H, Gibson NW, *et al.* Bioreductive activation of mitomycin C by DT-diaphorase. *Biochemistry* 1992; **31**:7879–7885.
9 Beall HD, Yafei L, Siegel D, Gibson NW, Ross D. Role of NAD(P)H:quinone oxidoreductase (DT-diaphorase) in cytotoxicity and induction of DNA damage by streptonigrin. *Biochem Pharmacol* 1996; **51**:645–652.
10 Cummings J, Ritchie A, Butler J, Ward TH, Langdon S. Activity profile of the novel aziridinylbenzoquinones MeDZQ and RH1 in human tumour xenografts. *Anticancer Res* 2003; **23**:3979–3983.
11 Siegel D, Gibson NW, Preusch PC, Ross D. Metabolism of diaziquone (AZQ) by NAD(P)H: (quinone-acceptor) oxidoreductase (DT-diaphorase): role in AZQ-induced DNA damage and cytotoxicity in human colon carcinoma cells. *Cancer Res* 1990; **50**:7293–7300.
12 Fisher GR, Gutierrez PL. The reductive metabolism of diaziquone (AZQ) in the S9 fraction of MCF-7 cells: free radical formation and NAD(P)H:quinone-acceptor oxidoreductase (DT-diaphorase) activity. *Free Rad Biol Med* 1991; **10**:359–370.
13 Cresteil T, Jaiswal AK. High levels of expression of the NAD(P)H:quinone oxidoreductase (NQO1) gene in tumor cells compared to normal cells of the same origin. *Biochem Pharmacol* 1991; **42**:1021–1027.
14 Jarrett CM, Bibby MC, Phillips RM. Bioreductive enzymology of malignant and normal human tissues. *Proc Am Ass Cancer Res* 1998; **39**:429–436.
15 Beall HD, Murphy AM, Siegel D, Hargreaves RHJ, Butler J, Ross D. Nicotinamide adenine dinucleotide (phosphate): quinone oxidoreductase (DT-diaphorase) as a target for bioreductive antitumor quinones: quinone cytotoxicity and selectivity in human lung and breast cancer cell lines. *Mol Pharmacol* 1995; **48**:499–504.
16 Winski SL, Hargreaves RHJ, Butler J, Ross D. A new screening system for NAD(P)H:quinone oxidoreductase (NQO1)-directed antitumor quinones: identification of a new aziridinylbenzoquinone, RH1, as a NQO1-directed antitumor agent. *Clin Cancer Res* 1998; **4**:3083–3088.
17 Dehn DL, Winski SL, Ross D. Development of a new isogenic cell-xenograft system for evaluation of NAD(P)H:quinone oxidoreductase-directed antitumor quinones: evaluation of the activity of RH1. *Clin Cancer Res* 2004; **10**:3147–3155.
18 Khan P, Abbas S, Hargreaves HJ, Caffrey R, Megram V, McGown A. Development and validation of a sensitive solid-phase extraction and high-performance liquid chromatographic assay for the novel bio-reductive anti-tumor agent RH1 in human and mouse plasma. *J Chromatogr B* 1999; **729**: 287–295.
19 Loadman PM, Phillips RM, Lim LE, Bibby MC. Pharmacological properties of a new aziridinylbenzoquinone, RH1 (2,5-diaziridinyl-3-(hydroxymethyl)-6-methyl-1,4-benzoquinone), in mice. *Biochem Pharmacol* 2000; **59**: 831–837.
20 Sharp SY, Kelland LR, Valenti MR, Brunton LA, Hobbs S, Workman P. Establishment of an isogenic human colon tumor model for NQO1 gene expression: application to investigate the role of DT-diaphorase in bioreductive drug activation *in vitro* and *in vivo*. *Mol Pharmacol* 2000; **58**:1146–1155.
21 Faing M, Bianchet MA, Winski S, Hargreaves R, Moody CJ, Hudnott RA, *et al.* Structure-based development of anticancer drugs: complexes of NAD(P)H:quinone oxidoreductase 1 with chemotherapeutic quinones. *Structure* 2001; **9**:659–667.
22 Winski SL, Swann E, Hargreaves RHJ, Dehn DL, Butler J, Moody CJ, *et al.* Relationship between NAD(P)H:quinone oxidoreductase 1 (NQO1) levels in a series of stably transfected cell lines and susceptibility to antitumor quinones. *Biochem Pharmacol* 2001; **61**:1509–1516.
23 Cheung AP, Struble E, Nguyen N, Liu P. Stability-indicating HPLC assay and solution stability of a new diaziridinyl benzoquinone. *J Pharm Biochem Anal* 2001; **24**:957–966.
24 Elliot MA, Ford SJ, Walker AA, Hargreaves RHJ, Halbert GW. Development of a lyophilised RH1 formulation: a novel DT diaphorase activated alkylating agent. *Pharm Pharmacol* 2001; **54**:487–492.
25 Nemeikaite-Ceniene AN, Sarlauskas J, Anusevicius Z, Nivinskas H, Cenas N. Cytotoxicity of RH1 and related aziridinylbenzoquinones: involvement of activation by NAD(P)H:quinone oxidoreductase (NQO1) and oxidative stress. *Arch Biochem Biophys* 2003; **416**:110–118.
26 Hargreaves RHJ, Hartley JA, Butler J. Mechanisms of action of quinone-containing alkylating agents aziridinylquinones. *Front Biosci* 2000; **5**: 172–180.
27 Xing C, Skibo EB. Sigmatropic reactions of the aziridinyl semiquinone species. Why aziridinyl benzoquinones are metabolically more stable than aziridinyl indoloquinones. *Biochemistry* 2000; **39**:10770–10780.

28 Fitzsimmons SA, Workman P, Grever M, Paull K, Camalier R, Lewis AD. Reductase enzyme expression across the National Cancer Institute tumor cell line panel: correlation with sensitivity to mitomycin C and EO9. *J Natl Cancer Inst* 1996; **88**:259–269.
29 Phillips RM. Bioreductive activation of a series of analogues of 5-aziridinyl-3-hydroxymethyl-1-methyl-2-[1H-indole-4,7-dione] pro-beta-en-alpha-ol (EO9) by human DT-diaphorase. *Biochem Pharmacol* 1996; **52**:1711–1718.
30 Tudor G, Gutierrez P, Aguilera-Gutierrez A, Sausville EA. Cytotoxicity and apoptosis of benzoquinones: redox cycling, cytochrome *c* release, and BAD protein expression. *Biochem Pharmacol* 2003; **65**:1061–1075.
31 Monks A, Scudiero D, Skehan P, Shoemaker R, Paull K, Vistica D, *et al.* Feasibility of a high-flux anticancer drug screen using a diverse panel of cultured human tumor cell lines. *J Natl Cancer Inst* 1991; **83**:757–766.
32 Monks A, Scudiero DA, Johnson GS, Paull KD, Sausville EA. The NCI anti-cancer drug screen: a smart screen to identify effectors of novel targets. *Anticancer Drug Des* 1997; **12**:533–541.
33 Alley MC, Scudiero DA, Monks A, Hursey ML, Czerwinski MJ, Fine DL, *et al.* Feasibility of drug screening with panels of human tumor lines using a microculture tetrazolium assay. *Cancer Res* 1988; **48**:589–601.
34 Alley MC, Pacula-Cox CM, Hollingshead MG, Camalier RF, Mayo JG, Plowman J, *et al.* Utility of a PVDF filter plate assay to facilitate selection of tumor cell lines for *in vivo* drug testing. *Proc Am Ass Cancer Res* 1995; **36**:305.
35 Hollingshead MG, Alley MC, Kaur G, Pacula-Cox CM, Stinson SF. Specialized *in vitro*/*in vivo* procedures employed by NCI In pre-clinical drug evaluations. In: Teacher BA, Andrews P (editors): *Anticancer Drug Development Guide: Preclinical Screening, Clinical Trials, and Approval*, 2nd edn. Totowa, NJ: Humana Press; 2005, in press.
36 Powis G. Metabolism and reactions of quinoid anticancer agents. *Pharmacol Ther* 1987; **35**:57–162.
37 Gutierrez PL. The metabolism of quinone-containing alkylating agents: free radical production and measurement. *Front Biosci* 2000; **5**:629–638.
38 Mossoba MM, Alizadeh M, Gutierrez PL. Mechanism for the reductive activation of Diaziquone. *J Pharm Sci* 1985; **74**:1249–1254.
39 Soldani C, Lazze MC, Bottone MG, Tognon G, Biggiogera M, Pellicciari CE, *et al.* Poly(ADP-ribose) polymerase cleavage during apoptosis: when and where? *Exp Cell Res* 2001; **269**:193–201.
40 Wardman P. Electron transfer and oxidative stress as key factors in the design of drugs selectively active in hypoxia. *Curr Med Chem* 2001; **8**:739–761.
41 Fourie J, Guziec Jr F, Guziec L, Monterrosa C, Fiterman DJ, Begleiter A. Structure–activity study with bioreductive benzoquinon alkylating agents: effects on DT-diaphorase-mediated DNA crosslink and strand break formation in relation to mechanism of cytotoxicity. *Cancer Chemother Pharmacol* 2004; **53**:191–203.
42 Tang DG, Zhenyu Zhu LL, Joshi B. Apoptosis in the absence of cytochrome *c* accumulation in the cytosol. *Biochem Biophys Res Commun* 1998; **242**:380–384.
43 Inayat-Hussain SH, Winski SL, Ross D. Differential involvement of caspases in hydroquinone-induced apoptosis in human leukemic HL-60 and Jurkat cells. *Toxicol Appl Pharmacol* 2001; **175**:95–103.